

Multi-latent Space Alignments for Unsupervised Domain Adaptation in Multi-view 3D Object Detection

Jiaming Liu^{1,*}, Rongyu Zhang^{1,2,*}, Xiaowei Chi³, Xiaoqi Li¹,
Ming Lu¹, Yandong Guo⁴, Shanghang Zhang^{1†}

¹Peking University, ²The Chinese University of Hong Kong, Shenzhen,

³The Chinese University of Hong Kong, ⁴Beijing University of Posts and Telecommunications

Abstract

Vision-Centric Bird-Eye-View (BEV) perception has shown promising potential and attracted increasing attention in autonomous driving. Recent works mainly focus on improving efficiency or accuracy but neglect the domain shift problem, resulting in severe degradation of transfer performance. With extensive observations, we figure out the significant domain gaps existing in the scene, weather, and day-night changing scenarios and make the first attempt to solve the domain adaption problem for multi-view 3D object detection. Since BEV perception approaches are usually complicated and contain several components, the domain shift accumulation on multi-latent spaces makes BEV domain adaptation challenging. In this paper, we propose a novel Multi-level Multi-space Alignment Teacher-Student (M^2ATS) framework to ease the domain shift accumulation, which consists of a Depth-Aware Teacher (DAT) and a Multi-space Feature Aligned (MFA) student model. Specifically, DAT model adopts uncertainty guidance to sample reliable depth information in target domain. After constructing domain-invariant BEV perception, it then transfers pixel and instance-level knowledge to student model. To further alleviate the domain shift at the global level, MFA student model is introduced to align task-relevant multi-space features of two domains. To verify the effectiveness of M^2ATS , we conduct BEV 3D object detection experiments on four cross domain scenarios and achieve state-of-the-art performance (e.g., +12.6% NDS and +9.1% mAP on Day-Night). Code and dataset will be released.

1. Introduction

The camera-based 3D object detection has attracted increasing attention, especially in the field of autonomous driving [2, 11, 12]. Nowadays, it has obtained obvious advancements driven by Bird-Eye-View (BEV) perception methods [24, 27–29, 42] and large scale labeled autonomous driving datasets [6, 19, 50]. However, due to the vast variety of perception scenes [31, 54], the camera-based methods can suffer significant performance degradation caused by domain shift or data distribution variation.

Recently, though mono-view 3D detection methods [30, 31] carry out the UDA setting on camera parameters or annotation methods variation, domain adaptation problem on many real-world scenarios is still unexplored in both Mono-view [5, 8, 15, 32, 48, 53, 61] and Multi-view [10, 24, 26, 28, 29, 33, 35, 36, 42, 43, 55] settings. As shown in Fig. 1, we discover the tremendous domain gap in the scene, weather, and day-night changing scenarios from source to target data in nuscnescenes [6], which leads to inferior performance of baseline [29] (only 0.174, 0.159, and 0.05 NDS). Therefore, we

attempt to transfer a multi-view 3D detector from a labeled source domain to an unlabeled target domain.

In UDA, the main challenge for Multi-view LSS-based BEV perception is the entangle of domain shift on multiple latent spaces: (1) *2D images latent space*. Since multi-view images contain abundant semantic information, it will result in a manifold domain shift when scenarios change. (2) *3D voxel latent space*. Voxel features that are constructed by domain-specific images feature and unreliable depth prediction will assemble more domain shift. (3) *BEV latent space*. Due to the shift in the above aspects, the constructed BEV feature results in an accumulation of domain shift and leading to alignment noises. As shown in Fig. 1 (a), we visualize the distribution of BEV features, which are obviously separated by domains on different cross domain scenarios.

To this end, we propose a novel Multi-level Multi-space Alignment Teacher-Student (M^2ATS) framework to disentangle domain shift problems in multiple latent spaces, which consists of a Depth-Aware Teacher (DAT) model and Multi-space Feature Aligned (MFA) Student model. DAT introduces composite depth-aware information to construct better voxel and BEV features in the target domain, which contains less source domain specific information. To con-

*Equal contribution: liujiaming@bupt.edu.cn

†Corresponding author: shzhang.pku@gmail.com

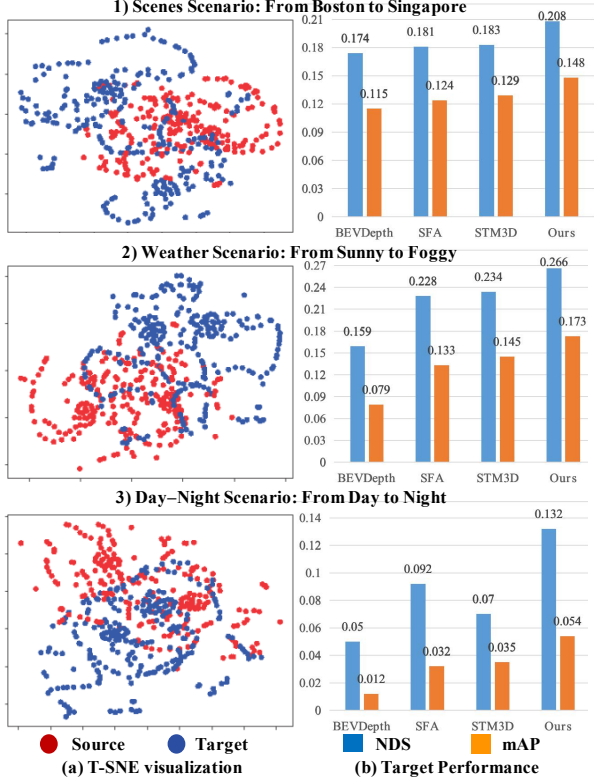


Figure 1. (a) T-SNE [52] visualization of the BEV features in different UDA scenarios, in which features are obviously separated by domain. (b) The performance of our method compared with previous works [29, 31, 54]. Both methods are built on BevDepth with a ResNet-50 backbone and evaluated on the target domain.

struct composite depth-aware information, DAT adaptively screened out reliably predicted depth by uncertainty estimation to compensate for lidar. It promotes representation consistency between DAT and student model through transferring domain-invariant multi-space knowledge and pseudo labels, thus addressing domain shift in pixel and instance level respectively. In order to assist DAT in further bridging global level domain gaps on multiple latent spaces, we propose MFA in the student model. It aligns three task-relevant features of two domains, including multi-view images, 3D voxel, and BEV features. In the overall M^2ATS framework, DAT and MFA compensate each other to address the domain shift of multiple latent spaces in multi-level.

As far as we know, we are the first to study the cross domain problem in Multi-View 3D object detection. We design three classical and one continual changing UDA scenarios, which are **Scene** (from Boston to Singapore), **Weather** (from sunny to rainy and foggy), **Day-night**, and **Changing Foggy degree** in [6]. For continual changing scenarios, we construct cross domain experiments with the continuously increased density of Fog, which gradually enlarges the domain gap. Our proposed method achieves competitive performance in all scenarios (shown in Fig. 1 (b)).

Compared with the previous state-of-the-art (SOTA) UDA method (i.e., STM3D [31]), it improves the NDS by 2.5, 3.2, and 5.2% respectively in three classical scenarios.

The main contributions are summarized as follows:

1) We explore the unsupervised domain adaptation (UDA) problem for BEV perception of Multi-view 3D object detection. We propose a novel Multi-level Multi-space Alignment Teacher-Student (M^2ATS) framework to address multi-latent space domain shift.

2) In M^2ATS , we propose a Depth-Aware Teacher (DAT) to construct uncertainty-guided depth-aware information, and then transfer the domain-invariant pixel-level features and instance-level pseudo label to the student model. M^2ATS contains a Multi-space Feature Aligned (MFA) student model which aligns multi-space features between two domains and compensates DAT to further alleviate the domain shift at global-level.

3) We conduct extensive experiments on the four challenging UDA scenarios, achieving SOTA performance compared with previous Mono-view 3D and 2D detection UDA methods. And we provide a Foggy-nuScene dataset.

2. Related work

2.1. Camera-based 3D object detection

Nowadays, 3D Object Detection plays an important role in autonomous driving and machine scene understanding. Two paradigms are prominent in this aspect: Single-view [3, 5, 8, 15, 32, 37, 40, 48, 53, 61] and Multi-view [10, 23, 24, 26–29, 33, 35, 36, 42, 43, 55]. In Single-view detection, previous works can be categorized into several streams, i.e. leveraging CAD models [3, 37, 40], setting prediction targets as key points [32, 61], and disentangling transformation for 2D and 3D detection [48]. Specifically, FCOS3D [53] can predict 2D and 3D attributes synchronously. M3D-RPN [5] considers single-view 3D object detection task as a standalone 3D region proposal network. In order to establish a more reliable 3D structure, D4LCN [15] alters 2D depth prediction with pseudo LiDAR representation. [8] calculates the depth of the objects by integrating the actual height of the objects. To better leverage the depth information in the detection process, MonoDTR [25] proposes an end-to-end depth-aware transformer network. However, taking into account the precision and practicality of detection, more and more multi-view 3D object detectors are proposed.

The Multi-view paradigm can be categorized into two branches, namely transformer-based [9] and LSS-based [42]. First of all, to extend DETR [9] into 3D detection, DETR3D [55] first predicts 3D bounding boxes with a transformer network. Inspired by DETR3D, some works adopt object queries [10, 26, 35, 36] or BEV grid queries [33] to extract features from images and utilize attention method, resulting in better 2D-to-3D transformation. How-

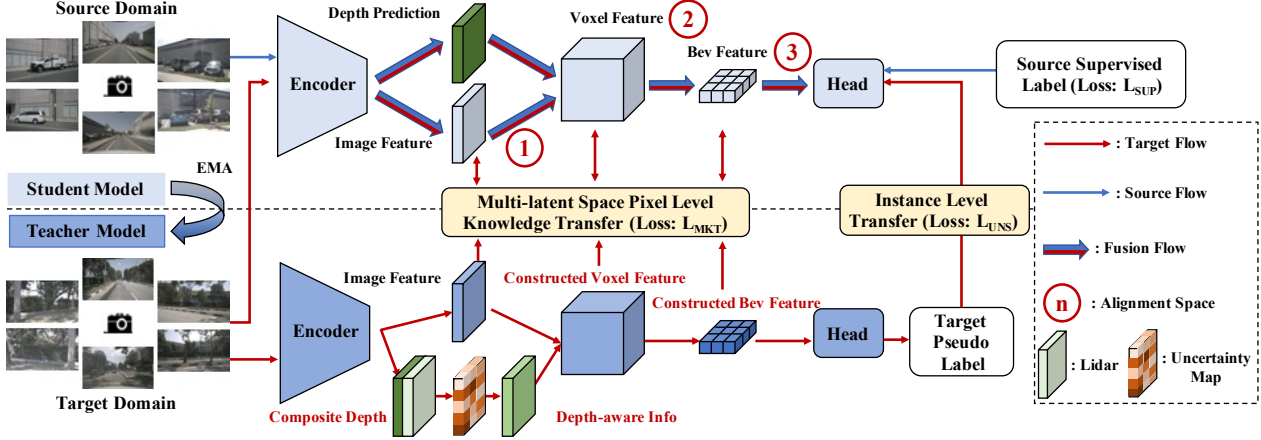


Figure 2. The framework of Multi-level Multi-space Alignment Teacher-Student (M^2ATS), which is composed of the Depth-Aware Teacher (DAT) and Multi-space Feature Aligned (MFA) student model. In the **bottom part**, the DAT model takes target domain input and adopts depth-aware information to construct domain-invariant features, which transfers pixel (multi-space features) along with instance-level (pseudo label) knowledge to the student model. In the **upper part**, the MFA student model aligns multi-space features (red circle) at the global level between two domains. M^2ATS framework aims to comprehensively address the multi-latent space domain shift problem.

ever, transformer-based methods don't project image features onto BEV representation. Following LSS [42], some methods [24, 28, 43] predict a distribution over lidar depth and generate a point cloud with multi-view image features for 3D detection. Specifically, BevDepth [29] introduces depth supervision and speeds up the operation of voxel pooling. Bevdet4d [23] and BevStereo [27] thoroughly explore temporal information in the task and concatenate volumes from multiple time steps. In this paper, we adopt BevDepth [29] as the baseline 3D object detector for its simple and powerful working flow, along with its great potential in cross domain feature extraction.

2.2. UDA in 3D object detection

Domain Adaptive Faster R-CNN [13] first probes the cross domain problem in object detection. Based on [17], most previous works [7, 45, 54, 56, 57, 59] follow the cross domain alignment strategy and explore the influence of domain shift in multi-level features. As for 3D object detection, [31, 39, 60] investigate Unsupervised Domain Adaptation (UDA) strategies for point cloud 3D detectors. In particular, [39, 60] adopt alignment methods to align the feature and instance level information between two domains. STM3D [31] develop self-training strategies to realize UDA by consistent and high-quality pseudo labels. Recently, some works [1, 4, 41, 47] investigate the cross domain strategies in BEV perception, which aim to reduce the simulation-to-real domain shift. In terms of camera-based monocular 3d object detection, [30, 31] first attempt to disentangle the camera parameters and guarantee the geometry consistency in cross domain phase. In contrast, we dedicate ourselves to solving the domain gap in multi-view 3d object detection tasks, which infer 3D scenes from the BEV perspective. We propose a novel Multi-level Multi-space

Alignment Teacher-Student framework to deal with the accumulation of domain shift on multi-latent spaces.

3. Methods

3.1. Overall framework

In this paper, we study the Unsupervised Domain Adaptation (UDA) problem in LSS-based Vision-Centric Bird-Eye-View (BEV) perception [29, 42], where the accumulation of multi-latent space domain shift existed. As shown in Fig. 2, **Multi-level Multi-space Alignment Teacher-Student (M^2ATS)** framework contains a Depth-Aware Teacher (DAT) and Multi-space Feature Aligned (MFA) Student model. Along with transferring multi-latent space knowledge from DAT to the student model, the MFA student model simultaneously aligns the task-relevant features between two domains in the same latent spaces. We discuss each component and its interactions in the following.

Depth-Aware Teacher model. As shown in Fig. 2, DAT extracts features and generates pseudo label from the target domain data, and transfers the pixel and instance-level knowledge to the student model. Specifically, due to the unreliable depth prediction and sparse property of target lidar, it suffers domain shift and incompleteness when constructing voxel and BEV features. Therefore, we introduce a depth-aware mechanism that completes the sparse lidar by the predicted depth and adopts uncertainty estimation to reserve reliable depth prediction. DAT then adopts depth-aware information as an intermediate to construct domain-invariant voxel and BEV features and generates reliable pseudo labels to fully exploit target domain data. The goal is to align the representation of DAT and the student model, thus alleviating domain shift accumulation.

Multi-space Feature Aligned student model. As shown

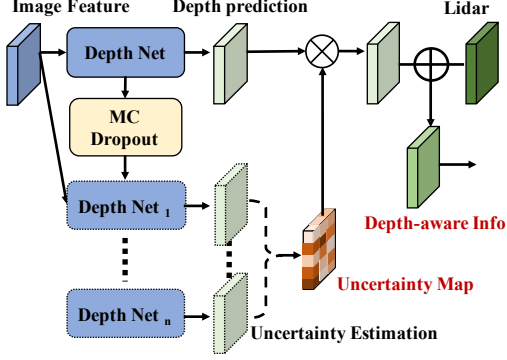


Figure 3. The detailed process of constructing depth-aware information. The uncertainty map is estimated by MC Dropout [16].

in Fig. 2, the MFA student model receives the transferred knowledge and deals with domain shift at the global level. It extracts features from both source and target domains while introducing an alignment mechanism to pull close the representation of two domains in multi-latent space. The alignments lie in the 2D image, voxel, and BEV features, which aim to obtain domain-invariant features and alleviate domain shift at global level. MFA and DAT compensate each other to address the domain shift in the same latent spaces.

3.2. Preliminary

For the UDA setting [62], we are provided by labeled source domain $D_s = \{\{I_s^i\}_{i=1}^M, L_s^i, G_s^i\}_{i=1}^{N_s}$ and unlabeled target domain $D_t = \{\{I_t^i\}_{i=1}^M, L_t^i\}_{i=1}^{N_t}$ of N samples and M camera views, in which I^i , L^i , and G^i denote images, lidar, and detection ground truth respectively. We adopt an encoder [22] to extract image features, and use lidar data L^i to supervise its depth prediction. These joint projects to 3D voxel feature VF^i , which are then voxel pooled to BEV feature BF^i . Note that, we only utilize lidar supervision during training following previous camera-based works [29].

3.3. Depth-aware teacher

Since detection perception is generated from voxel and BEV features which are initially constructed by depth prediction, the performance depends heavily on the accuracy of the depth sub-network estimation [27, 29]. However, cross domain transferring significantly aggravating depth prediction error [34]. Therefore, in Depth-Aware Teacher (DAT) model, our goal is to leverage depth-aware information to construct domain-invariant depth information along with corresponding voxel and BEV features.

To this end, we construct composite depth information in the teacher model by combining sparse lidar data with reliable and domain-invariant depth prediction. Note that, domain shift lies in the original depth prediction of the target domain, we thus adaptively screened out reliable prediction of the target domain by depth uncertainty estimation. In contrast to uncertainty guidance, a more simple

selection mechanism, which selects based on confidence score, moves decision boundaries to low-density regions in sampling-based approaches. However, it may lead to inaccuracy due to the poor calibration of neural networks. Moreover, the domain gap issue will result in more severe miscalibration [21]. Therefore, we adopt Dropout methods [16, 20] with uncertainty measurement instead of confidence predictions. Specifically, similar to [44], instead of designing a particular uncertainty measure, we pioneering introduce uncertainty guidance to ignore depth prediction of the source domain specified. And we offer a new solution to address the domain shift in dense prediction task, which leverages an uncertainty map to select reliable and domain-invariant pixel prediction in the target domain. When utilizing reliable depth information to build the following features in the target, the source data trained model has a better feature representation and concentrates more on depth estimation tasks without domain shift influence. The uncertainty map of depth prediction is:

$$D_{map}^i = \begin{cases} 1, & \mathcal{U}(D^i) \leq \mathcal{E}_{thresh} \\ 0, & \mathcal{U}(D^i) \geq \mathcal{E}_{thresh} \end{cases} \quad (1)$$

where $\mathcal{U}(D^i)$ is the uncertainty of i^{th} pixel depth prediction, and \mathcal{E}_{thresh} is the selected threshold, which is decided on the variance of the uncertainty values. As shown in Fig.3, we utilize an uncertainty map to obtain reliable depth prediction and composite target sparse Lidar data, constructing depth-aware information.

Inspired by the prevalent soft teacher [49, 58], the rest of the teacher model is built with mean teacher mechanism [51]. The weights of teacher model \mathcal{T}_{DAT} at time step t is the exponential moving average (EMA) of successive student model \mathcal{S}_{TGT} , shown below:

$$\mathcal{T}_{DAT}^t = \alpha \mathcal{T}_{DAT}^{t-1} + (1 - \alpha) \mathcal{S}_{TGT}^t \quad (2)$$

, where α is a smoothing coefficient. With the help of depth-aware information and mean-teacher mechanism, the DAT model can continuously transfer multi-latent space (*i.e.*, images, voxel, BEV, output) knowledge to the student, including pixel-level features and instance-level pseudo labels. The student model thus can concentrate more on task-driven knowledge learning without domain shift.

3.4. Multi-space feature aligned student

In student model learning, aside from the pixel and instance-level transferred knowledge from DAT, we further introduce Multi-space Feature Alignment (MFA) method to deal with the domain shift at the global level. In order to further alleviate the domain specific feature influence, we pull close the features representation of the source and target domain in multiple latent spaces, including 2D images, voxel, and BEV. Specifically, we utilize the domain adversarial training method [18] which inserts gradient reversal

layers and reverses back-propagated gradients for domain discriminators to optimize the model and extract domain-invariant features. Different from the previous alignment method [54, 59], LSS-based approaches hold multi-space features so that we align multi-space global information synchronously. The MFA loss \mathcal{L}_{MFA} is shown in Eq.3, where $F_{s,l}$ and $F_{t,l}$ is the source and target domain features at l latent space ($L \in \{images, voxel, BEV\}$) and D denotes the domain discriminator.

$$\mathcal{L}_{MFA}(F_s, F_t) = \sum_{l \in L} (\log D(F_{s,l}) + \log(1 - D(F_{t,l}))) \quad (3)$$

In the M^2ATS framework, DAT and MFA compensate each other to deal with the multi-latent spaces domain shift problem in multi-level.

3.5. Training objectives and inference

The M^2ATS framework contains a Depth-Aware Teacher (DAT) model and Multi-space Feature Aligned (MFA) Student model, the teacher model is updated by EMA operation. When adopting the DAT model to transfer multi-space features to the student, the knowledge transfer loss \mathcal{L}_{MKT} is shown as follows:

$$\mathcal{L}_{MKT} = \sum_{l \in L} \frac{1}{W'_l \times H'_l} \sum_{i \in \mathcal{P}} \|F_{Te,l}^i - F_{St,l}^i\|^2 \quad (4)$$

where $F_{Te,l}^i$ and $F_{St,l}^i$ stand for the i^{th} pixel value from DAT model and student model at l latent space, $L \in \{images, voxel, BEV\}$. W'_l and H'_l stand for width and height of the transferred features, $\mathcal{P} = \{1, 2, \dots, W'_l \times H'_l\}$. We thus pull close the distance of the feature between model \mathcal{T}_{DAT} and \mathcal{S}_{TGT} with MSE loss. With the help of pixel-level domain-invariant knowledge transfer, we can reduce the domain shift in the three latent spaces. Meanwhile, the integrated domain adaptation loss \mathcal{L}_{DA} is shown in Eq.5.

$$\mathcal{L}_{DA} = \lambda_1 * \mathcal{L}_{UNC} + \lambda_2 * \mathcal{L}_{MKT} + \lambda_3 * \mathcal{L}_{MFA} \quad (5)$$

, where \mathcal{L}_{UNC} is the detection loss [29] penalized by target domain pseudo label, which is generated by teacher model. In order to maintain the balance of loss penalties, λ_1 is set to 1, λ_2 and λ_3 is set to 0.1. During inference, same with other camera-based methods [27, 29, 33], we only adopt multi-view camera data.

4. Evaluation

We conduct extensive experiments to demonstrate the effectiveness of the Multi-level Multi-space Alignment Teacher-Student (M^2ATS) framework. In Sec 4.1, the details of the setup of UDA scenarios and implementation details are given. In Sec 4.2, we evaluate the cross domain performance of M^2ATS in the three classical and

one continual changing scenarios, including scene, weather, day-night, and continuously increased foggy degree Adaptation. The comprehensive ablation studies are conducted in Sec 4.3, which investigate the impact of each component. Finally, we provide qualitative analysis to better present the effectiveness of our proposed framework in Sec 4.4.

4.1. Experimental setup

4.1.1 Datasets and adaptation scenarios

We evaluate our proposed framework on nuscenets [6], which is a large-scale autonomous-driving dataset. In order to pave the way for Unsupervised Domain Adaptation (UDA) in multi-view 3d object detection, we split the nuscenets into different paired source-target domain data. We introduce three classical and challenging cross-domain scenarios, which are **Scene**, **Weathers**, and **Day-Night** adaptation. In addition, Due to the lack of foggy weather (a normal target data), we generate a foggy dataset (Foggy-nuscenets) in various dense degrees inspired by Foggy-Cityscapes [46]. The Foggy-nuscenets dataset will be released for research. Besides, we also evaluate M^2ATS in the continual changing scenario of increased foggy degrees.

Scene Adaptation We set Boston as the source scene data and realize UDA on the Singapore target domain. Since scene layouts are frequently changing in autonomous driving, the domain gap occurs in multiple scenes.

Weathers Adaptation The sunny weather is considered as source domain data, rainy and foggy weather is considered as target domain data. Various weather conditions are common phenomena in the real world, and multi-view 3d object detection should be reliable under such conditions.

Day-Night Adaptation We design daytime data as the source domain and realize UDA on the target domain (night data). Since the camera-based method has a tremendous domain gap from day to night, it is essential to explore the domain adaptation method in the day-night scenario.

Continues Changing Adaptation We set sunny weather data as the source domain and set continuously increased foggy degree data as the target domain. Specifically, we realize UDA from sunny to Foggy-1, Foggy-3, and Foggy-5 step by step with the degree of fog increased. Since the continual changing domain gap usually appears in autonomous driving, the domain shift is essential to be addressed. Moreover, we demonstrate the detailed information and generation method of the dataset in the appendix.

4.1.2 Implementation details

M^2ATS framework is built based on BEVDepth [29]. According to previous work [24, 28, 29, 43], ResNet-50 and ResNet-101 [22] serve as backbone to extract image features respectively. We adopt 256×704 as image input size and the same data augmentation methods as [29]. We apply

Table 1. Results of different methods for scene adaptation scenario on the validation set [6], from Boston to Singapore. DA means utilizing the domain adaption method, and R50 and R101 adopt Resnet 50 and 101 as the backbone.

	Method	Backbone	NDS ↑	mAP ↑	mATE ↓	mASE ↓	MAOE ↓	mAVE ↓	mAAE ↓
Baseline	BEVDet [24]	R50	0.126	0.117	0.873	0.787	1.347	1.302	0.666
	BEVDepth [29]	R50	0.174	0.115	0.888	0.412	1.031	1.056	0.527
	BEVDepth [29]	R101	0.187	0.115	0.874	0.391	0.944	1.021	0.501
DA	SFA [54](BEVDepth)	R50	0.181	0.124	0.856	0.411	1.023	1.075	0.540
	STM3D [31](BEVDepth)	R50	0.183	0.129	0.840	0.421	1.050	1.055	0.550
DA	Ours(BEVDepth)	R50	0.208	0.148	0.813	0.402	0.907	1.134	0.536
	Ours(BEVDepth)	R101	0.211	0.166	0.758	0.427	1.127	1.108	0.535

Table 2. Results of different methods for weather adaptation scenarios on the validation set [6], from Sunny to Rainy and Foggy-3.

	Method	Backbone	Target Rainy			Target Foggy-3		
			NDS ↑	mAP ↑	mATE ↓	NDS ↑	mAP ↑	mATE ↓
Baseline	BEVDet [24]	R50	0.232	0.207	0.818	0.135	0.072	0.867
	BEVDepth [29]	R50	0.268	0.196	0.824	0.159	0.079	0.882
	BEVDepth [29]	R101	0.272	0.212	0.842	0.202	0.122	0.804
DA	SFA [54](BEVDepth)	R50	0.281	0.200	0.840	0.228	0.133	0.840
	STM3D [31](BEVDepth)	R50	0.276	0.212	0.820	0.234	0.145	0.721
DA	Ours(BEVDepth)	R50	0.305	0.243	0.819	0.266	0.173	0.805
	Ours(BEVDepth)	R101	0.308	0.247	0.726	0.271	0.174	0.793

AdamW [38] optimizer with $2e-4$ learning rate and without any decay. For training, the source domain pretrain and UDA experiments are trained for 24 and 12 epochs **without CBGS** [63]. During inference, our method infers without any test time augmentation or model ensemble. We report the evaluation metrics following previous 3d detection works [24, 29], including nuScenes Detection Score (NDS), mean Average Precision (mAP), as well as five True Positive (TP) metrics including mean Average Translation Error (mATE), mean Average Scale Error (mASE), mean Average Orientation Error (MAOE), mean Average Velocity Error (mAVE), mean Average Attribute Error (mAAE). All experiments are conducted on NVIDIA Tesla V100 GPUs.

4.2. Main results

We compare our proposed method with other BEV perception methods to verify the superior performance of M^2ATS . Meanwhile, to further demonstrate our special design in addressing domain shift of LSS-based multi-view 3D object detection, we reproduce other promising 2D and mono-view 3D detection Domain Adaptation (DA) methods on BEVDepth [29], *i.e.*, SFA [54] and STM3D [31].

Scene Adaptation As shown in Tab. 1, M^2ATS outperforms all the baseline methods, which obviously exceeds BEVDepth [29] of R50 and R101 backbone by 3.4% and 2.4% NDS. It thus demonstrates that our proposed method can effectively address the multi-latent spaces domain shift caused by scene and environmental change. Compared with other SOTA DA methods, M^2ATS outperforms SFA and STM3D by 2.7% and 2.5% NDS respectively. And it even

improves mAP by 1.9% compared with 2nd place. The comparison further demonstrates that our proposed method is specially designed for LSS-based 3D object detection.

Weathers Adaptation As shown in Tab. 2, in Sunny to Foggy-3 scenario adaptation, M^2ATS outperforms other baseline methods by a significant margin. It even exceeds BEVDepth by around 10% in both NDS and mAP (R50 setting). Moreover, compared with SFA and STM3D, M^2ATS improves NDS by 3.8% and 3.2% respectively since it utilizes multi-space domain invariant features to realize a better representation in extreme weather data. In order to evaluate the generalization of M^2ATS , we also conduct experiments on Sunny to Rainy, M^2ATS also increases 2.4% NDS compared with 2nd place.

Day-Night Adaptation The Day-Night adaptation is the most challenging scenario for camera-based methods, M^2ATS significantly improves the detection performance and solves the domain shift problem in the Night domain. As shown in Tab. 3, the tremendous domain gap makes baseline methods perform extremely poorly with only 0.062 NDS and 0.036 mAP under R101. While M^2ATS , especially with R101 as its backbone, can achieve 0.188 NDS and 0.127 mAP. Even compared with other domain adaptation methods, it also achieves a superior improvement of more than 4.0% and 6.2%. Since previous DA methods like STM3D and STA ignore the inaccuracy depth estimation in Night data, it thus can not effectively deal with Day-Night domain shift in the LSS-based method.

Continues Changing Adaptation As shown in Tab. 4, due to the page limitation, we only compare M^2ATS with

Table 3. Results of different methods for day-night adaptation scenario on the validation set [6].

	Method	Backbone	NDS \uparrow	mAP \uparrow	mATE \downarrow	mASE \downarrow	mAOE \downarrow	mAVE \downarrow	mAAE \downarrow
Baseline	BEVDet [24]	R50	0.010	0.009	0.990	0.977	1.078	1.509	0.984
	BEVDepth [29]	R50	0.050	0.012	0.042	0.646	1.129	1.705	0.915
	BEVDepth [29]	R101	0.062	0.036	1.033	0.706	0.973	1.447	0.895
DA	SFA [54](BEVDepth)	R50	0.092	0.032	0.995	0.556	0.993	1.480	0.948
	STM3D [31](BEVDepth)	R50	0.070	0.035	0.979	0.549	1.063	1.587	0.937
DA	Ours(BEVDepth)	R50	0.132	0.054	0.711	0.465	1.072	1.504	0.772
	Ours(BEVDepth)	R101	0.188	0.127	0.189	0.484	0.820	1.784	0.711

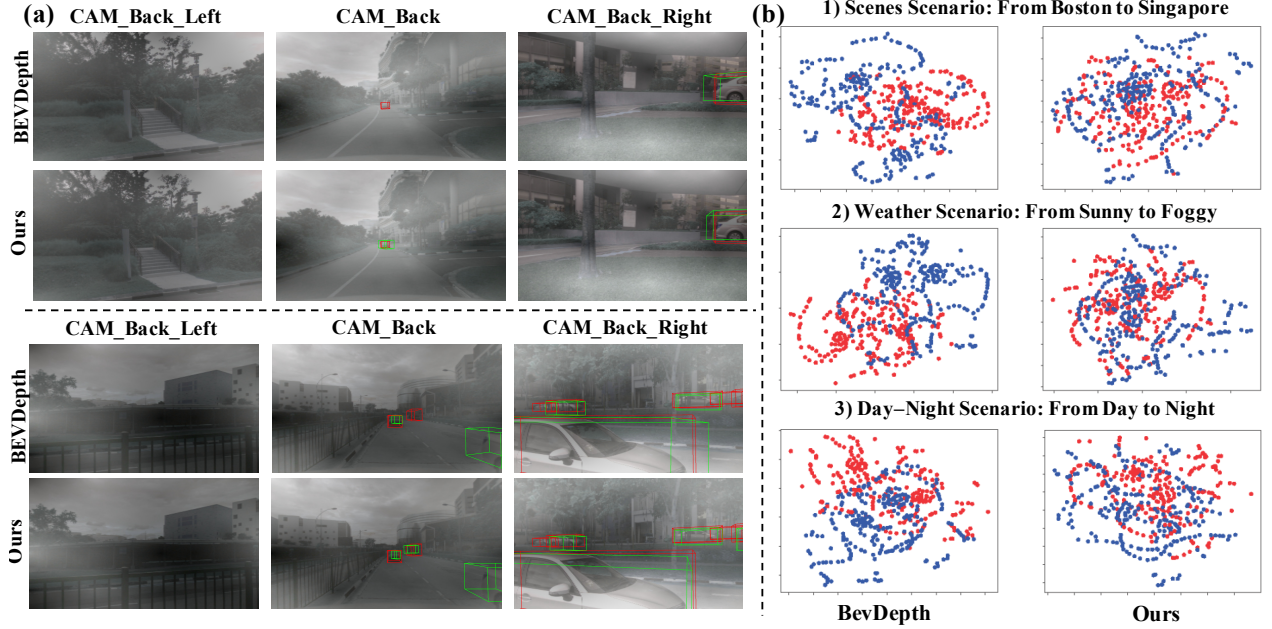


Figure 4. Visualizations on the benefits of our proposed method. (a) Qualitative results: The upper and bottom parts are visualization of BevDepth [29] and our proposed method respectively. The results are visualized on the weather adaptation scenario. (b) Visualization of feature distributions using T-SNE [52]. The blue spots denote the source features, while red spots represent target features.

Table 4. Results of different methods for continuous changing adaptation scenario on Nuscenes-Foggy, from Sunny to Foggy-1, Foggy-3, and Foggy-5 step by step. The metric is NDS

Train on	Method(R50)	Foggy-1	Foggy-3	Foggy-5
Sunny	BEVDepth [29]	0.2214	0.1592	0.096
	Ours(BEVDepth)	0.2835	0.2728	0.2190

the baseline method. Along with the increased foggy degree, the baseline method shows an obvious performance degradation. However, M^2ATS alleviates the gradually increased domain gap and outperforms the baseline method by 12.3% NDS in the final Foggy-5 domain.

4.3. Ablation study

To better reflect the role of each component in M^2ATS , we conduct ablation experiments to analyze how each component can deal with domain shift for LSS-based BEV perception. It should be noted that the ablation study is only

conducted on **Sunny-Rainy** weather adaptation. The ablation study of other scenarios is presented in the appendix.

The effectiveness of DAT and MFA. As shown in Tab. 5, vanilla BEVDepth (Ex_0) can only achieve 26.8% NDS and 19.6% mAP when the scenario is transformed from sunny to the rainy domain. For DAT, it transfers multi-latent space knowledge to the student model via domain invariant multi-space features and more reliable pseudo labels, which are constructed by depth-aware information. As shown in Ex_1 , the student model can learn pixel and instance level knowledge from DAT, NDS, and mAP are improved by 1.5% and 3.5% respectively. Ex_2 evaluates the benefits of mean-teacher mechanism, achieving further 0.4% mAP improvement. By gradually aligning the multi-space feature (Ex_{3-5}) in the student model, our method will get a 2% improvement in NDS, which demonstrates that it is essential to align the global-level representation of two domains in multi-latent spaces. When we combine DAT and MFA in M^2ATS (Ex_{6-7}), NDS can be further enhanced to 30.5%

Table 5. Ablation studies on the Sunny to Rainy scenario. It shows the effectiveness of DAT and MFA in the framework. For DAT, it consists of three components, including depth-aware information(DA), mean-teacher(MT), and multi-latent space knowledge transfer(KT). For MFA, it concludes three-latent space alignments, which are Bev(BA), image(IA), and voxel(VA) feature alignment.

Name	DA	MT	KT	BA	IA	VA	NDS \uparrow	mAP \uparrow
Ex_0	-	-	-	-	-	-	0.268	0.196
Ex_1	✓	-	✓	-	-	-	0.283	0.231
Ex_2	✓	✓	✓	-	-	-	0.286	0.235
Ex_3	-	-	-	✓	-	-	0.276	0.200
Ex_4	-	-	-	✓	✓	-	0.282	0.204
Ex_5	-	-	-	✓	✓	✓	0.288	0.207
Ex_6	✓	-	✓	✓	✓	✓	0.301	0.238
Ex_7	✓	✓	✓	✓	✓	✓	0.305	0.243

Table 6. The ablation study on the effectiveness of each component in depth-aware information. Pred means depth prediction, and UG means adaptive uncertainty-guided depth selection.

Depth-aware:	Lidar	Pred	UG	NDS \uparrow	mAP \uparrow
Ex_{2-1}	✓	-	-	0.275	0.223
Ex_{2-2}	✓	✓	-	0.278	0.228
Ex_2	✓	✓	✓	0.286	0.235

Table 7. The ablation study on the effectiveness of each component in Multi-latent space Knowledge Transfer. PL means transferring instance-level pseudo labels. BEV, Voxel, and Image stand for transferring on corresponding latent spaces.

Latent Space:	PL	BEV	Voxel	Image	NDS \uparrow	mAP \uparrow
Ex_{2-3}	✓	-	-	-	0.280	0.213
Ex_{2-4}	✓	✓	-	-	0.283	0.222
Ex_{2-5}	✓	✓	✓	-	0.285	0.230
Ex_2	✓	✓	✓	✓	0.286	0.235

while mAP can achieve 24.3%. We can come to the conclusion that NDS and mAP continuously increase with the addition of each component in DAT and MFA, demonstrating that each of these modules is necessary and effective. It also proves that DAT and MFA can compensate each other to address the domain shift in multi-latent spaces.

Detailed ablation study of DAT We study the effectiveness of depth-aware information composition and multi-latent knowledge transferring in DAT. As shown in Tab. 6, only taking lidar ground truth to replace depth prediction (Ex_{2-1}) can improve 0.7% NDS and 2.7% mAP compared with Ex_0 . The obviously increased mAP demonstrates that lidar data plays an important role in domain invariant voxel feature construction. However, due to the sparse property of lidar data, we utilize dense depth prediction to composite sparse lidar. In (Ex_{2-2}), NDS and mAP can achieve

27.9% and 22.8%, which only have limited improvement compared with Ex_{2-1} . Therefore, we introduce uncertainty guidance to adaptively select more reliable and task-relevant depth predictions. Ex_2 has obvious performance progress compared with Ex_{2-1} and Ex_{2-2} , demonstrating the uncertainty-guided depth selection can reduce the domain shift caused by domain specific depth prediction. As shown in Tab. 7, applying for knowledge transfer in different latent spaces can be beneficial to M^2ATS . With pseudo label, BEV, voxel, and image feature transferred between DAT and student model, NDS is gradually improved from 26.8% to 28.6%, and mAP is improved from 19.6% to 23.5%. The improved performance demonstrates that multi-space global-level alignment is introduced to ease different domain shifts in each latent space. It shows that pseudo label and three spaces knowledge are all essential for the student model to address multi-latent space domain gaps, which is constructed by depth-aware information.

4.4. Qualitative analysis

We further present some visualization results of the prediction produced by the M^2ATS and the baseline BEVDpeth [29], as shown in Fig. 4 (a). It is quite clear that the BEVDpeth fails to locate the objects well, while M^2ATS yields more accurate localization results as its predicted **green box** overlaps better with the ground truth **red box**. We can also observe that M^2ATS can detect objects that baseline ignores, demonstrating the superiority of M^2ATS in object detection and presenting great potential in deploying to real-world autonomous driving applications. The visualization in Fig. 4 (b) further verifies the explicit cross domain ability of M^2ATS . As a clear separation can be seen in the clusters of the **blue-source** and **red-target** dots produced by BEVDpeth, the features generated by M^2ATS get closer together further demonstrates the ability of our proposed method in representing domain invariant features.

5. Conclusion and discussion of limitations

We explore the UDA problem in Multi-View 3D object detection and propose a novel Multi-level Multi-space Alignment Teacher-Student (M^2ATS) framework to fully ease multi-latent space domain shift for LSS-based BEV perception. On the one hand, Depth-Aware Teacher (DAT) leverages depth-aware information to generate reliable pseudo labels and multi-space domain-invariant features, which are transferred to the student model. On the other hand, the Multi-space Feature Aligned (MFA) student model utilizes source and target domain data to align the global-level feature representation. M^2ATS achieves SOTA performance in three challenge UDA and continual changing domain gap scenarios. For limitations, the teacher-student framework brings more computational cost and extra small parameters (discriminator) during training.



Figure 5. The visualization of Foggy-Nuscenes dataset. The first row is the original multi-view images in Nuscenes [6], and the last three rows demonstrate images of increased foggy degree.

However, the student model keeps the same forward time and computational cost with a baseline in inference.

6. Appendix

In the supplementary material, we first present more details of our generated Foggy Nuscenes dataset in Sec .6.1, which aims at adding a foggy weather scene in Nuscenes [6] and providing an open source dataset (Foggy-Nuscenes) for research in autonomous driving. Secondly, in Sec .6.2, we show the details of each scenario and the partition of dataset. In Sec .6.3, we then provide additional and detailed cross domain training strategy. In Sec .6.4, the extra ablation studies are conducted on Day-night cross-domain scenario, which investigate the impact of each component in the Multi-level Multi-space Alignment Teacher-Student (M^2ATS) framework. Finally, we provide additional qualitative analysis on Day-night scenario to further evaluate the effectiveness of our proposed method in Sec 6.5.

6.1. Supplementary description of foggy Nuscenes dataset

We apply the fog simulation pipeline [46] to the multi-view images provided in the Nuscenes dataset [6]. specifically, we generate synthetic foggy images for all scenes of training, validation, and test set, which reserve original annotation of 3D object detection task. We utilize five different density degree of foggy simulator to construct Foggy-Nuscenes dataset, including Foggy-1, Foggy-2, Foggy-3, Foggy-4, and Foggy-5 (gradually increasing fog density). As shown in Fig .5, we adopt Foggy-1, Foggy-3, and Foggy-5 as the experimental datasets for weather adaptation and continual changing scenario, which have an obvious domain gap with original Nuscenes dataset [6].

6.2. Additional details of UDA scenarios

In this paper, we utilize Nuscenes [6] and Foggy-Nuscenes datasets to generate three classical and one continual changing UDA scenarios. As shown in Tab .8, for Scene changing scenario, We set Boston as the source scene data and realize UDA on the Singapore target domain. The source domain contains 15.6k frames labeled data and target domain has 12.4k frames unlabeled data. For Weather changing scenario, the sunny weather is considered as source domain data, rainy and foggy weather is considered as target domain data. In the second row, the source domain has 1276 training sequences and rainy target domain has 274 training sequences. In the third row, we leverage all Nuscenes dataset as source domain data and set Foggy-3 as target domain data. As we can see, in Day-night changing scenario, we design daytime data as the source domain and realize UDA on the target domain (night data). Since the source domain data is way more larger than the target domain data and the camera can not capture night-time data clearly, which is considered as the most challenging adaptation scenarios. Finally, we set all Nuscenes sequence as the source domain data and set continuously increased foggy degree data as the target domain. The various target domains are of the same sequence and scene with source domain, but the different foggy degree on the frames bring significant domain gap. We introduce this continual changing scenario to demonstrate the continual domain adaptation ability of our proposed method.

6.3. Additional implementation details

Our training process of cross domain can be divided into 2 stages: pretraining on source domain and transfer training from source to target domain. Firstly, in order to fully

Table 8. The partitioning and details of four UDA scenarios. Frames means the number of multi-view image frames in the datasets.

UDA scenarios	Domain	Training sequences	Frames	Validation sequences	Frames
Scene changing	Source(Boston)	857	15695	77	3090
	Target(Singapore)	693	12435	73	2929
Weather changing	Source(Sunny)	1276	23070	126	5051
	Target(Rainy)	274	5060	24	968
Weather changing	Source(Nuscenes)	1550	28130	150	6019
	Target(Foggy-3)	1550	28130	150	6019
Day-night changing	Source(Day)	1367	24745	135	5417
	Target(Night)	183	3385	15	602
Continual changing	Source(Nuscenes)	1550	28130	150	6019
	Target-1(Foggy-1)	1550	28130	150	6019
	Target-2(Foggy-3)	1550	28130	150	6019
	Target-3(Foggy-5)	1550	28130	150	6019

Table 9. Ablation studies on the Day-night scenario. It shows the effectiveness of DAT and MFA in the framework. For DAT, it consists of three components, including depth-aware information(DA), mean-teacher(MT), and multi-latent space knowledge transfer(KT). For MFA, it concludes three-latent space alignments, which are Bev(BA), image(IA), and voxel(VA) feature alignment.

Name	DA	MT	KT	BA	IA	VA	NDS \uparrow	mAP \uparrow
Ex_0	-	-	-	-	-	-	0.050	0.012
Ex_1	✓	-	✓	-	-	-	0.103	0.034
Ex_2	✓	✓	✓	-	-	-	0.104	0.041
Ex_3	-	-	-	✓	-	-	0.065	0.038
Ex_4	-	-	-	✓	✓	-	0.071	0.042
Ex_5	-	-	-	✓	✓	✓	0.098	0.051
Ex_6	✓	-	✓	✓	✓	✓	0.124	0.049
Ex_7	✓	✓	✓	✓	✓	✓	0.132	0.054

leverage the feature extraction ability of the model [29], we load the backbone of ImageNet [14] pretrained parameters. Then we train the model on the source domain data in a supervised manner, which aims to obtain the source domain pretrained model parameters. In cross domain phase, we load the integrated model parameters, which are pretrained on source domain, into the student model and conduct transferred training for 12 epochs. M^2ATS framework adopts source domain and target domain data as input, and only leverages source domain annotation. During training, we alternate Depth-Aware Teacher knowledge transferred and Multi-space Feature Alignment training to update student model. Finally, we directly infer the student model on target domain data and achieve the result of our proposed method.

6.4. Additional ablation study on day-night scenario

The M^2ATS framework contains a Depth-Aware Teacher (DAT) and a Multi-space Feature Aligned (MFA) student model. To evaluate each component of the proposed

Table 10. The ablation study on the effectiveness of each component in depth-aware information. Pred means depth prediction, and UG means adaptive uncertainty-guided depth selection.

Depth-aware:	Lidar	Pred	UG	NDS \uparrow	mAP \uparrow
Ex_{2-1}	✓	-	-	0.068	0.028
Ex_{2-2}	✓	✓	-	0.084	0.032
Ex_2	✓	✓	✓	0.104	0.041

Table 11. The ablation study on the effectiveness of each component in Multi-latent space Knowledge Transfer. PL means transferring instance-level pseudo labels. BEV, Voxel, and Image stand for transferring on corresponding latent space.

Latent Space:	PL	BEV	Voxel	Image	NDS \uparrow	mAP \uparrow
Ex_{2-3}	✓	-	-	-	0.076	0.036
Ex_{2-4}	✓	✓	-	-	0.096	0.039
Ex_{2-5}	✓	✓	✓	-	0.101	0.044
Ex_2	✓	✓	✓	✓	0.104	0.041

M^2ATS framework, we conduct ablation experiments to analyze how each component can mitigate domain shift for LSS-based BEV perception. It should be noted that the ablation study is conducted on the most challenging **Day-Night** scenario, in which other methods suffer tremendous performance degradation.

The effectiveness of DAT and MFA. As shown in Tab. 9, due to the faint light of target domain (night-time), vanilla BEVDepth (Ex_0) can only achieve 5.0% NDS and 1.2% mAP when the scenario is transformed from source domain (daytime). For DAT, it transfers multi-latent space knowledge to the student model via pixel-level multi-space features and instance-level pseudo labels, which are constructed by depth-aware information. As shown in Ex_1 , the student model can learn domain-invariant knowledge from DAT, NDS and mAP are thus improved by 5.3% and 2.2%

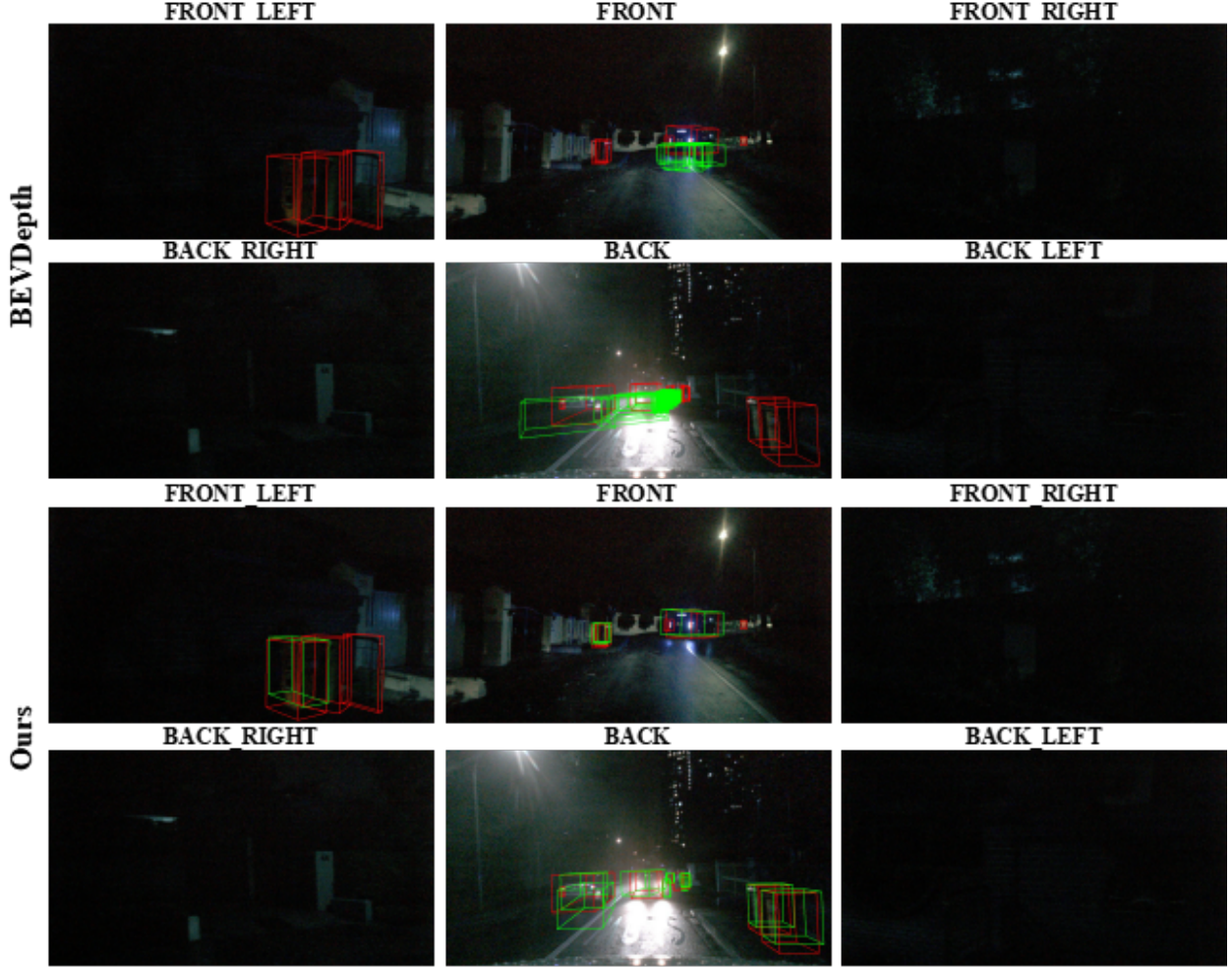


Figure 6. Visualizations on the benefits of our proposed method. The upper and bottom parts are visualization of BeVDepth [29] and our proposed method respectively. The red box is the Ground Truth, and the green box is the predictions.

respectively. Ex_2 evaluates the benefits of mean-teacher mechanism, which brings 0.7% mAP improvement. As we can see, depth-aware information plays an important role in cross domain transferred learning and greatly improves NDS compared with baseline. By gradually aligning the multi-space feature (Ex_{3-5}) in the MFA student model, our method get a 4.8% and 3.9% improvement in NDS and mAP, which demonstrates that it is essential to align the global-level representation of two domains in multi-latent spaces. The MFA student model has a great improvement on mAP compared with baseline, in which the global-level alignment focuses more on classification and location of objects. When we combine DAT and MFA in M^2ATS (Ex_{6-7}), NDS can be further enhanced to 13.2% while mAP can achieve 5.4%. We can come to the conclusion that NDS and mAP continuously increase with the addition of each component in DAT and MFA, showing similar results with the previous ablation study on submission. It also

proves that DAT and MFA can compensate each other to address the domain shift in multi-latent spaces.

Detailed ablation study of DAT We study the effectiveness of depth-aware information composition and multi-latent knowledge transferring in DAT. As shown in Tab. 10, only taking lidar ground truth to replace depth prediction (Ex_{2-1}) can only improve 1.8% NDS and 1.6% mAP compared with BEVDepth (Ex_0). The obviously increased performance demonstrates that lidar data plays an important role in domain-invariant voxel feature construction. However, due to the sparse property of lidar data, we utilize dense depth prediction to composite sparse lidar data. In (Ex_{2-2}), NDS and mAP can achieve 8.4% and 3.2%, which only have limited improvement compared with Ex_{2-1} . Therefore, we introduce uncertainty guidance to adaptively select more reliable and task-relevant depth predictions to composite sparse lidar data. Due to the reliable composite depth-aware information, Ex_2 has obvi-

ous performance progress compared with Ex_{2-2} , which further improves 2.0% NDS and 0.9% mAP. The results demonstrate the uncertainty-guided depth selection can reduce the domain shift caused by domain specific depth prediction. As shown in Tab. 11, applying knowledge transfer on different latent spaces can be beneficial to M^2ATS . With pseudo label, BEV, voxel, and image feature transferred between DAT and student model, NDS is gradually improved from 5.0% to 10.4%, and mAP is improved from 1.2% to 4.1%. The results show that pseudo label and the knowledge of three spaces are all essential for the student model to address multi-latent space domain gaps, which is constructed by depth-aware information. In conclusion, leveraging depth-aware information has a significant impact on addressing multi-space domain shift in BEV perception, which transfers domain-invariant knowledge from teacher model to student model.

6.5. Additional qualitative analysis

In contrast with the visualization on submission, we further present some visualization results of the prediction produced by the M^2ATS and the baseline BEVDpeth [29] on the most challenging scenario (day-night), as shown in Fig. 6. Due to the faint light of night-time data, we can not classify and locate objects even with the naked eye, not to mention camera-based methods. It is quite clear that the BEVDpeth has various inaccurate and missing detection, while M^2ATS yields more accurate localization results as its predicted **green box** overlaps better with the ground truth **red box**. We can also observe that M^2ATS can detect objects that baseline ignores, demonstrating the superiority of M^2ATS in object detection and presenting great potential in deploying to real-world autonomous driving applications. However, our proposed method still has some missing detection which inspires us to pay more attention on the BEV perception in night-time.

References

- [1] David Acuna, Jonah Philion, and Sanja Fidler. Towards optimal strategies for training self-driving perception models in simulation. *Advances in Neural Information Processing Systems*, 34:1686–1699, 2021. 3
- [2] Eduardo Arnold, Omar Y Al-Jarrah, Mehrdad Dianati, Saber Fallah, David Oxtoby, and Alex Mouzakitis. A survey on 3d object detection methods for autonomous driving applications. *IEEE Transactions on Intelligent Transportation Systems*, 20(10):3782–3795, 2019. 1
- [3] Ivan Barabanau, Alexey Artemov, Evgeny Burnaev, and Vyacheslav Murashkin. Monocular 3d object detection via geometric reasoning on keypoints. *arXiv preprint arXiv:1905.05618*, 2019. 2
- [4] Alejandro Barrera, Jorge Beltrán, Carlos Guindel, Jose Antonio Iglesias, and Fernando García. Cycle and semantic consistent adversarial domain adaptation for reducing simulation-to-real domain shift in lidar bird’s eye view. In *2021 IEEE International Intelligent Transportation Systems Conference (ITSC)*, pages 3081–3086. IEEE, 2021. 3
- [5] Garrick Brazil and Xiaoming Liu. M3d-rpn: Monocular 3d region proposal network for object detection. In *Proceedings of the IEEE/CVF International Conference on Computer Vision*, pages 9287–9296, 2019. 1, 2
- [6] Holger Caesar, Varun Bankiti, Alex H Lang, Sourabh Vora, Venice Erin Liong, Qiang Xu, Anush Krishnan, Yu Pan, Giancarlo Baldan, and Oscar Beijbom. nuscenes: A multi-modal dataset for autonomous driving. In *Proceedings of the IEEE/CVF conference on computer vision and pattern recognition*, pages 11621–11631, 2020. 1, 2, 5, 6, 7, 9
- [7] Qi Cai, Yingwei Pan, Chong-Wah Ngo, Xinmei Tian, Lingyu Duan, and Ting Yao. Exploring object relation in mean teacher for cross-domain detection. In *Proceedings of the IEEE/CVF Conference on Computer Vision and Pattern Recognition*, pages 11457–11466, 2019. 3
- [8] Yingjie Cai, Buyu Li, Zeyu Jiao, Hongsheng Li, Xingyu Zeng, and Xiaogang Wang. Monocular 3d object detection with decoupled structured polygon estimation and height-guided depth estimation. In *Proceedings of the AAAI Conference on Artificial Intelligence*, volume 34, pages 10478–10485, 2020. 1, 2
- [9] Nicolas Carion, Francisco Massa, Gabriel Synnaeve, Nicolas Usunier, Alexander Kirillov, and Sergey Zagoruyko. End-to-end object detection with transformers. In *European conference on computer vision*, pages 213–229. Springer, 2020. 2
- [10] Shaoyu Chen, Xinggang Wang, Tianheng Cheng, Qian Zhang, Chang Huang, and Wenyu Liu. Polar parametrization for vision-based surround-view 3d detection. *arXiv preprint arXiv:2206.10965*, 2022. 1, 2
- [11] Xiaozhi Chen, Kaustav Kundu, Ziyu Zhang, Huimin Ma, Sanja Fidler, and Raquel Urtasun. Monocular 3d object detection for autonomous driving. In *Proceedings of the IEEE conference on computer vision and pattern recognition*, pages 2147–2156, 2016. 1
- [12] Xiaozhi Chen, Huimin Ma, Ji Wan, Bo Li, and Tian Xia. Multi-view 3d object detection network for autonomous driving. In *Proceedings of the IEEE conference on Computer Vision and Pattern Recognition*, pages 1907–1915, 2017. 1
- [13] Yuhua Chen, Wen Li, Christos Sakaridis, Dengxin Dai, and Luc Van Gool. Domain adaptive faster r-cnn for object detection in the wild. In *Proceedings of the IEEE conference on computer vision and pattern recognition*, pages 3339–3348, 2018. 3
- [14] Jia Deng, Wei Dong, Richard Socher, Li-Jia Li, Kai Li, and Li Fei-Fei. Imagenet: A large-scale hierarchical image database. In *2009 IEEE conference on computer vision and pattern recognition*, pages 248–255. Ieee, 2009. 10
- [15] Mingyu Ding, Yuqi Huo, Hongwei Yi, Zhe Wang, Jianping Shi, Zhiwu Lu, and Ping Luo. Learning depth-guided convolutions for monocular 3d object detection. In *Proceedings of the IEEE/CVF Conference on Computer Vision and Pattern Recognition Workshops*, pages 1000–1001, 2020. 1, 2
- [16] Yarin Gal and Zoubin Ghahramani. Dropout as a bayesian approximation: Representing model uncertainty in deep

- learning. In *international conference on machine learning*, pages 1050–1059. PMLR, 2016. 4
- [17] Yaroslav Ganin and Victor Lempitsky. Unsupervised domain adaptation by backpropagation. In *International conference on machine learning*, pages 1180–1189. PMLR, 2015. 3
- [18] Yaroslav Ganin, Evgeniya Ustinova, Hana Ajakan, Pascal Germain, Hugo Larochelle, François Laviolette, Mario Marchand, and Victor Lempitsky. Domain-adversarial training of neural networks. *The journal of machine learning research*, 17(1):2096–2030, 2016. 4
- [19] Andreas Geiger, Philip Lenz, and Raquel Urtasun. Are we ready for autonomous driving? the kitti vision benchmark suite. In *2012 IEEE conference on computer vision and pattern recognition*, pages 3354–3361. IEEE, 2012. 1
- [20] Golnaz Ghiasi, Tsung-Yi Lin, and Quoc V Le. Dropblock: A regularization method for convolutional networks. *Advances in neural information processing systems*, 31, 2018. 4
- [21] Chuan Guo, Geoff Pleiss, Yu Sun, and Kilian Q Weinberger. On calibration of modern neural networks. In *International conference on machine learning*, pages 1321–1330. PMLR, 2017. 4
- [22] Kaiming He, Xiangyu Zhang, Shaoqing Ren, and Jian Sun. Deep residual learning for image recognition. In *Proceedings of the IEEE conference on computer vision and pattern recognition*, pages 770–778, 2016. 4, 5
- [23] Junjie Huang and Guan Huang. Bevdet4d: Exploit temporal cues in multi-camera 3d object detection. *arXiv preprint arXiv:2203.17054*, 2022. 2, 3
- [24] Junjie Huang, Guan Huang, Zheng Zhu, and Dalong Du. Bevdet: High-performance multi-camera 3d object detection in bird-eye-view. *arXiv preprint arXiv:2112.11790*, 2021. 1, 2, 3, 5, 6, 7
- [25] Kuan-Chih Huang, Tsung-Han Wu, Hung-Ting Su, and Winston H Hsu. Monodtr: Monocular 3d object detection with depth-aware transformer. In *Proceedings of the IEEE/CVF Conference on Computer Vision and Pattern Recognition*, pages 4012–4021, 2022. 2
- [26] Yanqin Jiang, Li Zhang, Zhenwei Miao, Xiatian Zhu, Jin Gao, Weiming Hu, and Yu-Gang Jiang. Polarformer: Multi-camera 3d object detection with polar transformers. *arXiv preprint arXiv:2206.15398*, 2022. 1, 2
- [27] Yinhao Li, Han Bao, Zheng Ge, Jinrong Yang, Jianjian Sun, and Zeming Li. Bevstereo: Enhancing depth estimation in multi-view 3d object detection with dynamic temporal stereo. *arXiv preprint arXiv:2209.10248*, 2022. 1, 2, 3, 4, 5
- [28] Yanwei Li, Yilun Chen, Xiaojuan Qi, Zeming Li, Jian Sun, and Jiaya Jia. Unifying voxel-based representation with transformer for 3d object detection. *arXiv preprint arXiv:2206.00630*, 2022. 1, 2, 3, 5
- [29] Yinhao Li, Zheng Ge, Guanyi Yu, Jinrong Yang, Zengran Wang, Yukang Shi, Jianjian Sun, and Zeming Li. Bevdepth: Acquisition of reliable depth for multi-view 3d object detection. *arXiv preprint arXiv:2206.10092*, 2022. 1, 2, 3, 4, 5, 6, 7, 8, 10, 11, 12
- [30] Zhenyu Li, Zehui Chen, Ang Li, Liangji Fang, Qinrong Jiang, Xianming Liu, and Junjun Jiang. Towards model generalization for monocular 3d object detection. *arXiv preprint arXiv:2205.11664*, 2022. 1, 3
- [31] Zhenyu Li, Zehui Chen, Ang Li, Liangji Fang, Qinrong Jiang, Xianming Liu, and Junjun Jiang. Unsupervised domain adaptation for monocular 3d object detection via self-training. *arXiv preprint arXiv:2204.11590*, 2022. 1, 2, 3, 6, 7
- [32] Zhuoling Li, Zhan Qu, Yang Zhou, Jianzhuang Liu, Haoqian Wang, and Lihui Jiang. Diversity matters: Fully exploiting depth clues for reliable monocular 3d object detection. In *Proceedings of the IEEE/CVF Conference on Computer Vision and Pattern Recognition*, pages 2791–2800, 2022. 1, 2
- [33] Zhiqi Li, Wenhai Wang, Hongyang Li, Enze Xie, Chonghao Sima, Tong Lu, Qiao Yu, and Jifeng Dai. Bevformer: Learning bird’s-eye-view representation from multi-camera images via spatiotemporal transformers. *arXiv preprint arXiv:2203.17270*, 2022. 1, 2, 5
- [34] Jiaming Liu, Qizhe Zhang, Jianing Li, Ming Lu, Tiejun Huang, and Shanghang Zhang. Unsupervised spike depth estimation via cross-modality cross-domain knowledge transfer. *arXiv preprint arXiv:2208.12527*, 2022. 4
- [35] Yingfei Liu, Tiancai Wang, Xiangyu Zhang, and Jian Sun. Petr: Position embedding transformation for multi-view 3d object detection. *arXiv preprint arXiv:2203.05625*, 2022. 1, 2
- [36] Yingfei Liu, Junjie Yan, Fan Jia, Shuailin Li, Qi Gao, Tiancai Wang, Xiangyu Zhang, and Jian Sun. Petrv2: A unified framework for 3d perception from multi-camera images. *arXiv preprint arXiv:2206.01256*, 2022. 1, 2
- [37] Zongdai Liu, Dingfu Zhou, Feixiang Lu, Jin Fang, and Liangjun Zhang. Autoshape: Real-time shape-aware monocular 3d object detection. In *Proceedings of the IEEE/CVF International Conference on Computer Vision*, pages 15641–15650, 2021. 2
- [38] Ilya Loshchilov and Frank Hutter. Decoupled weight decay regularization. *arXiv preprint arXiv:1711.05101*, 2017. 6
- [39] Zhipeng Luo, Zhongang Cai, Changqing Zhou, Gongjie Zhang, Haiyu Zhao, Shuai Yi, Shijian Lu, Hongsheng Li, Shanghang Zhang, and Ziwei Liu. Unsupervised domain adaptive 3d detection with multi-level consistency. In *Proceedings of the IEEE/CVF International Conference on Computer Vision*, pages 8866–8875, 2021. 3
- [40] Fabian Manhardt, Wadim Kehl, and Adrien Gaidon. Roi-10d: Monocular lifting of 2d detection to 6d pose and metric shape. In *Proceedings of the IEEE/CVF Conference on Computer Vision and Pattern Recognition*, pages 2069–2078, 2019. 2
- [41] Mong H Ng, Kaahan Radia, Jianfei Chen, Dequan Wang, Ionel Gog, and Joseph E Gonzalez. Bev-seg: Bird’s eye view semantic segmentation using geometry and semantic point cloud. *arXiv preprint arXiv:2006.11436*, 2020. 3
- [42] Jonah Philion and Sanja Fidler. Lift, splat, shoot: Encoding images from arbitrary camera rigs by implicitly unprojecting to 3d. In *European Conference on Computer Vision*, pages 194–210. Springer, 2020. 1, 2, 3
- [43] Cody Reading, Ali Harakeh, Julia Chae, and Steven L Waslander. Categorical depth distribution network for monocular 3d object detection. In *Proceedings of the*

- IEEE/CVF Conference on Computer Vision and Pattern Recognition*, pages 8555–8564, 2021. 1, 2, 3, 5
- [44] Mamshad Nayeem Rizve, Kevin Duarte, Yogesh S Rawat, and Mubarak Shah. In defense of pseudo-labeling: An uncertainty-aware pseudo-label selection framework for semi-supervised learning. *arXiv preprint arXiv:2101.06329*, 2021. 4
- [45] Kuniaki Saito, Yoshitaka Ushiku, Tatsuya Harada, and Kate Saenko. Strong-weak distribution alignment for adaptive object detection. In *Proceedings of the IEEE/CVF Conference on Computer Vision and Pattern Recognition*, pages 6956–6965, 2019. 3
- [46] Christos Sakaridis, Dengxin Dai, and Luc Van Gool. Semantic foggy scene understanding with synthetic data. *International Journal of Computer Vision*, 126(9):973–992, 2018. 5, 9
- [47] Khaled Saleh, Ahmed Abobakr, Mohammed Attia, Julie Iskander, Darius Nahavandi, Mohammed Hossny, and Saeid Nahvandi. Domain adaptation for vehicle detection from bird’s eye view lidar point cloud data. In *Proceedings of the IEEE/CVF International Conference on Computer Vision Workshops*, pages 0–0, 2019. 3
- [48] Andrea Simonelli, Samuel Rota Buló, Lorenzo Porzi, Manuel López-Antequera, and Peter Kotschieder. Disentangling monocular 3d object detection. In *Proceedings of the IEEE/CVF International Conference on Computer Vision*, pages 1991–1999, 2019. 1, 2
- [49] Kihyuk Sohn, Zizhao Zhang, Chun-Liang Li, Han Zhang, Chen-Yu Lee, and Tomas Pfister. A simple semi-supervised learning framework for object detection. *arXiv preprint arXiv:2005.04757*, 2020. 4
- [50] Pei Sun, Henrik Kretschmar, Xerxes Dotiwalla, Aurelien Chouard, Vijaysai Patnaik, Paul Tsui, James Guo, Yin Zhou, Yuning Chai, Benjamin Caine, et al. Scalability in perception for autonomous driving: Waymo open dataset. In *Proceedings of the IEEE/CVF conference on computer vision and pattern recognition*, pages 2446–2454, 2020. 1
- [51] Antti Tarvainen and Harri Valpola. Mean teachers are better role models: Weight-averaged consistency targets improve semi-supervised deep learning results. *Advances in neural information processing systems*, 30, 2017. 4
- [52] Laurens Van Der Maaten. Barnes-hut-sne. *arXiv preprint arXiv:1301.3342*, 2013. 2, 7
- [53] Tai Wang, Xinge Zhu, Jiangmiao Pang, and Dahua Lin. Fcos3d: Fully convolutional one-stage monocular 3d object detection. In *Proceedings of the IEEE/CVF International Conference on Computer Vision*, pages 913–922, 2021. 1, 2
- [54] Wen Wang, Yang Cao, Jing Zhang, Fengxiang He, Zheng-Jun Zha, Yonggang Wen, and Dacheng Tao. Exploring sequence feature alignment for domain adaptive detection transformers. In *Proceedings of the 29th ACM International Conference on Multimedia*, pages 1730–1738, 2021. 1, 2, 3, 5, 6, 7
- [55] Yue Wang, Vitor Campagnolo Guizilini, Tianyuan Zhang, Yilun Wang, Hang Zhao, and Justin Solomon. Detr3d: 3d object detection from multi-view images via 3d-to-2d queries. In *Conference on Robot Learning*, pages 180–191. PMLR, 2022. 1, 2
- [56] Chang-Dong Xu, Xing-Ran Zhao, Xin Jin, and Xiu-Shen Wei. Exploring categorical regularization for domain adaptive object detection. In *Proceedings of the IEEE/CVF Conference on Computer Vision and Pattern Recognition*, pages 11724–11733, 2020. 3
- [57] Minghao Xu, Hang Wang, Bingbing Ni, Qi Tian, and Wenjun Zhang. Cross-domain detection via graph-induced prototype alignment. In *Proceedings of the IEEE/CVF Conference on Computer Vision and Pattern Recognition*, pages 12355–12364, 2020. 3
- [58] Mengde Xu, Zheng Zhang, Han Hu, Jianfeng Wang, Lijuan Wang, Fangyun Wei, Xiang Bai, and Zicheng Liu. End-to-end semi-supervised object detection with soft teacher. In *Proceedings of the IEEE/CVF International Conference on Computer Vision*, pages 3060–3069, 2021. 4
- [59] Jinze Yu, Jiaming Liu, Xiaobao Wei, Haoyi Zhou, Yohei Nakata, Denis Gudovskiy, Tomoyuki Okuno, Jianxin Li, Kurt Keutzer, and Shanghang Zhang. Cross-domain object detection with mean-teacher transformer. *arXiv preprint arXiv:2205.01643*, 2022. 3, 5
- [60] Weichen Zhang, Wen Li, and Dong Xu. Srdan: Scale-aware and range-aware domain adaptation network for cross-dataset 3d object detection. In *Proceedings of the IEEE/CVF Conference on Computer Vision and Pattern Recognition*, pages 6769–6779, 2021. 3
- [61] Yunpeng Zhang, Jiwen Lu, and Jie Zhou. Objects are different: Flexible monocular 3d object detection. In *Proceedings of the IEEE/CVF Conference on Computer Vision and Pattern Recognition*, pages 3289–3298, 2021. 1, 2
- [62] Sicheng Zhao, Xiangyu Yue, Shanghang Zhang, Bo Li, Han Zhao, Bichen Wu, Ravi Krishna, Joseph E Gonzalez, Alberto L Sangiovanni-Vincentelli, Sanjit A Seshia, et al. A review of single-source deep unsupervised visual domain adaptation. *IEEE Transactions on Neural Networks and Learning Systems*, 2020. 4
- [63] Benjin Zhu, Zhengkai Jiang, Xiangxin Zhou, Zeming Li, and Gang Yu. Class-balanced grouping and sampling for point cloud 3d object detection. *arXiv preprint arXiv:1908.09492*, 2019. 6